Editors' Suggestion | Featured in Physics

Hohlraum Reheating from Burning NIF Implosions

M. S. Rubery,* M. D. Rosen, N. Aybar, O. L. Landen, L. Divol, C. V. Young, C. Weber, J. Hammer, J. D. Moody, A. S. Moore, A. L. Kritcher, A. B. Zylstra, O. Hurricane, A. E. Pak, S. MacLaren, G. Zimmerman, J. Harte, and T. Woods
Lawrence Livermore National Laboratory, P.O. Box 808, Livermore, California 94551-0808, USA

(Received 22 May 2023; accepted 4 December 2023; published 5 February 2024)

As fusion experiments at the National Ignition Facility (NIF) approach and exceed breakeven, energy from the burning capsule is predicted to couple to the gold walls and reheat the hohlraum. On December 5, 2022, experiment N221204 exceeded target breakeven, historically achieving 3.15 MJ of fusion energy from 2.05 MJ of laser drive; for the first time, energy from the igniting capsule reheated the hohlraum beyond the peak laser-driven radiation temperature of 313 eV to a peak of 350 eV, in less than half a nanosecond. This reheating effect has now been unambiguously observed by the two independent Dante calorimeter systems across multiple experiments, and is shown to result from reheating of the remnant tungsten-doped ablator by the exploding core, which is heated by alpha deposition.

DOI: 10.1103/PhysRevLett.132.065104

The inertial confinement fusion (ICF) program at the National Ignition Facility (NIF) [1–3] aims to achieve ignition via the spherically convergent compression of a deuterium-tritium (DT)-filled capsule using the indirect-drive approach [4–6]. During indirect drive, a gold hohlraum is driven by 192 NIF beams with a combined energy of ~2 MJ, to a radiation temperature in excess of $T_R = 300$ eV. At the center of the hohlraum, a 2 mm diameter capsule filled with DT gas, surrounded by a cryogenic DT ice layer and outer ablative layer of high-density carbon, is imploded by the rocket effect. Upon stagnation, it is compressed and heated to over 100 g/cm^3 and 100 million Kelvin, plasma conditions sufficiently hot and dense to initiate nuclear fusion.

Generating the hot spot conditions for a sustained alpha burn requires fine tuning many interdependent laser, hohlraum, and capsule design parameters. The combination implemented in the latest NIF experiments, specifically the Hybrid-E campaign in this note [7], represents 13 years of incremental changes to designs and experiments, and the careful diagnosis of the dominant failure modes across the hundreds of x-ray, particle, and photon diagnostics at NIF [7–15]. One such x-ray diagnostic, the Dante calorimetry system, has been used since the inception of NIF to monitor the interior radiation temperature T_R of the hohlraum [16–21].

Beginning with the record-breaking N210808 Hybrid-E shot in August 2021 [12,22,23], burning capsules at NIF have, for the first time, generated fusion products sufficient to reheat the hohlraum at times consistent with the nuclear bang time and with integral power that correlates well with the alpha component of the fusion energy. A year later in December 2022, a revised Hybrid-E design historically exceeded the input laser energy in shot N221204 [24–26], surpassing controlled fusion breakeven at a gain of 3.15 MJ/2.05 MJ = 1.5; a substantial hohlraum reheating signature was detected on both Dante systems. Fusion energy was observed to reheat the hohlraum well beyond the laser-driven peak radiation temperature of 313 eV to almost 350 eV for the first time. This rapidly assembled (< 1 ns) and unique thermal source ($T_R > 300$ eV), which is inaccessible anywhere else on Earth, may be used as a driver for future experiments in the high-energy density (HED) regime, such as opacity, dynamic strength, and equation of state. Furthermore, as we will demonstrate, the heating we observe from Dante originates solely from the alpha component of the fusion yield, without dependence on the neutron channel. No diagnostic at NIF has previously demonstrated this capability, and by understanding this phenomena we provide additional confidence to existing fusion yield calculations. In this report, we present the Dante measurements and analysis of the observed reheating signatures throughout 2021 and 2022, and discuss how alpha energy from the burning plasma is able to redrive the cooling hohlraum.

Two spectrally sensitive Dante calorimetry systems are employed at NIF. Each comprises 18 independent channels and contains a combination of L- and K-edge filters and planar reflection mode X-31 XRDs [27]; in lower energy channels, a grazing-incidence Bragg-reflecting mirror may be installed to reject higher-energy contamination. Dante 1 is located at $\theta = 143°$, $\phi = 274°$, where $\theta = 0°$ is defined in the vertical axis in Fig. 1(a), and is generally used as the primary diagnostic for radiation temperature owing to its favorable 37° view of the hohlraum laser-entrance hole (LEH) and three x-ray mirrors, which gives this line of sight increased sensitivity to the higher x-ray energies observed on indirect-drive ICF experiments, compared with Dante 2. The second Dante 2 system is located at $\theta = 64°$, $\phi = 350°$

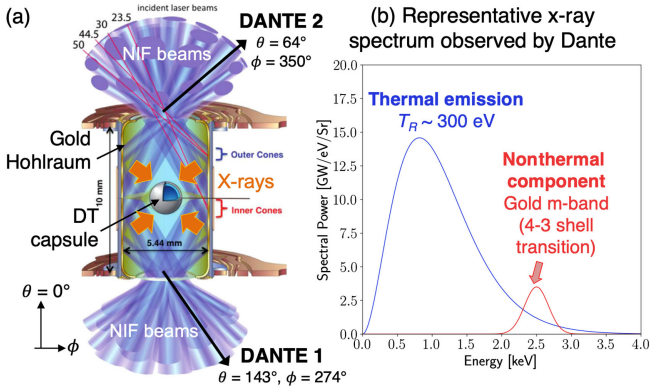

FIG. 1. (a) Schematic of a typical ICF experiment at NIF, where 192 beams heat the interior of a gold hohlraum to T_R~300 eV in order to compress a 2 mm DT capsule to the conditions required for fusion. (b) Representative hohlraum emission spectrum observed by the Dante calorimeter showing thermal region (blue) and gold *m*-band emission (red).

and has a more shallow view of the LEH compared with Dante 1. In addition, Dante 2 has 11 mirrored channels, giving the system comparably higher sensitivity at lower x-ray energies. Nonetheless, both Dantes are routinely deployed during ICF experiments for redundancy and consistency.

The timing accuracy of Dante, of critical importance to monitor the hohlraum's response to gradients and inflections in the laser pulse, *and recently the nuclear reheating signature*, is measured *insitu* during gold ball experiments. In these experiments, two quads of NIF laser energy in a 88 ps pulse are used to generate an x-ray timing signature observable across all channels. The signature is subsequently used to cross time each channel to the NIF timing system, with an accuracy of ±50 ps. Concomitantly, we can also recover the impulse response for each channel, which is well approximated by a ~400 ps wide Gaussian, and is dominated by the bandwidth of the signal cable [28] and XRD.

The traditional algorithm used to extract spectra from the 18 channel voltages is known locally as *UNSPEC* [29–32]. At each point in time, *UNSPEC* fits a Planckian to lower-energy channels; this shape is then iteratively perturbed using Gaussian approximations to the individual channel spectral responses until a good match is obtained between spectral solution and observed voltages. It is then trivial to extract flux and temperature histories by integrating the set of spectral solutions over time. When fully calibrated and optimally configured, the Dante systems combined with the *UNSPEC* algorithm, can report total flux F and radiation temperature T_R with 1σ uncertainties of 4% and 1.5%, respectively, at peak emission where digitizer noise can be considered small. A full description of the *UNSPEC* analysis methodology has been published previously.

Between August 2021 and December 2022, nine experiments from the Hybrid-E campaign [7] were conducted with fusion yields high enough to produce notable reheating of the hohlraum. Dante 1 and 2 flux histories are shown in Figs. 2(a) and 3(a). The NIF laser system consistently drove hohlraums in the series to a T_R of 313 eV with a standard deviation of ±2 eV, as observed by Dante 1, and $T_R = 308$ eV ± 3 eV from Dante 2. Throughout this report, flux from the latter have been corrected by 28% to compensate for an obstruction near the LEH. Radiation temperatures quoted are calculated using the Stefan-Boltzmann relation combined with the initial LEH dimensions. In practice, gold expansion throughout the drive will reduce the effective LEH area [33]; T_R values presented herein therefore represent a lower bound.

To conclusively attribute the reheating signature evident in Figs. 2(a) and 2(b) and 3(a) and 3(b) with a nuclear effect and for the phenomena to be practical, the measurement must scale in a clear and predictable way with fusion yield and contain integral energy consistent with the energetics of the burning capsule. Moreover, the arrival time must correlate with peak fusion reactivity. In order to test against these criteria, the heating component of the signal after the laser drive shuts off at 8 ns must be isolated from the emissions of the cooling hohlraum; this is achieved by fitting a power law to the flux before and after the onset of reheating. Figures 2(b) and 3(b) illustrate the methodology

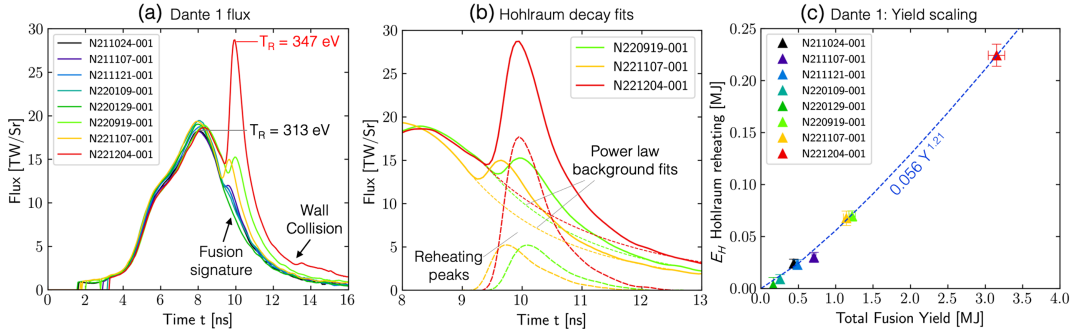

FIG. 2. (a) Dante 1 flux histories from the Hybrid-E shots in 2021 and 2022 showing clear fusion signature at approximately 10 ns. (b) A closer look at the reheating signatures illustrating the background subtraction and residuals for three of the higher yield experiments. (c) Integrated hohlraum reheating energy E_H calculated using Eq. (1) as a function of fusion yield.

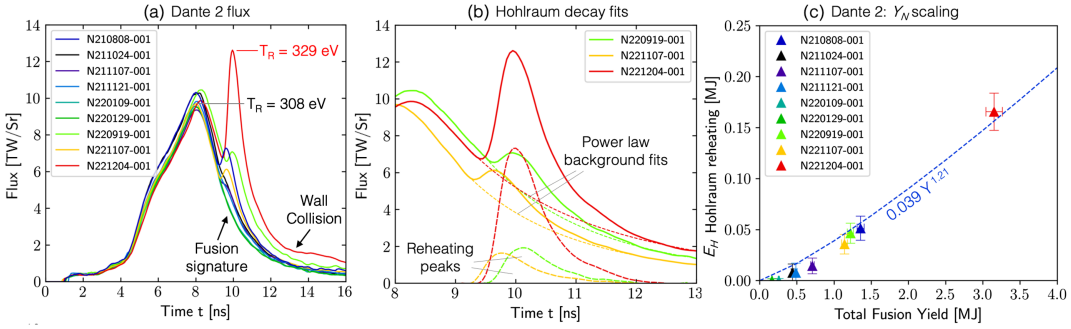

FIG. 3. (a) Dante 2 flux histories from the Hybrid-E shots in 2021 and 2022 showing clear fusion signature at approximately 10 ns. (b) A closer look at the reheating signatures illustrating the background subtraction and residuals for three of the higher yield experiments. (c) Integrated hohlraum reheating energy E_H calculated using Eq. (1) as a function of fusion yield.

for three of the most prominent heating signatures. The reheating component is then extracted by subtracting the background power law from the original flux.

A simple estimate of the internal hohlraum energy E_H can be made assuming the emission is Lambertian, and scaling by the surface viewable from Dante to the interior wall area inside the hohlraum:

$$E_H = \frac{\pi}{\cos\theta}\int_{t_1}^{t_2} F(t)\frac{((1-\alpha)A_{\text{wall}} + 2A_{\text{LEH}})}{A_{\text{LEH}}}dt, \quad (1)$$

where θ is the Dante view angle, $F(t)$ is Dante flux, A_{wall} is the effective wall area of the hohlraum and A_{LEH} is the area of the LEH as viewed by Dante. In order to simplify the expression of E_H we have assumed a constant wall albedo, $\alpha = 0.8$ throughout the reheating [34]. In reality, α is a complex quantity depending on temperature and plasma conditions, and varies with time; however, for gross comparison with fusion energetics the approximation is sufficient. Integrated hohlraum simulations, which include the latest physics models for the gold wall conditions, including albedo, are discussed later in this Letter.

Reheating energy E_H for the nine shots is plotted against fusion yield in Figs. 2(c) and 3(c) for Dante 1 and 2 respectively. Uncertainty in the reheating peak was obtained by combining uncertainties from x-ray calibration facilities [29] and rf components, with Monte Carlo calculations of the flux [30]. Fusion yields at NIF are traditionally measured using activation techniques [35–40]; in this analysis we use the uncertainty-weighted averages from the well NADS nuclear activation detectors [41], converted to total fusion energy Y by correcting for down-scatter ratio as measured by the magnetic recoil spectrometer and neutron time-of-flight diagnostics [42–44] and scaled additionally by $5/4$ to account for the alpha channel of the DT reaction.

If we fit scaling laws to Figs. 2(c) and 3(c), we find that $\kappa Y^{1.21}$ fits the data well, with $\kappa = 0.056$ and 0.039 for Dante 1 and 2 respectively, with Y in units of MJ. Dante 1 has a favorable view of the hohlraum waist near to the burning capsule, which may explain its larger value of κ; in addition, deviation from ideal Lambertian emission may also influence the magnitude of κ from each line of sight.

Taking a closer look at record performer N221204, we obtain a reheating energy E_H of 220 ± 30 kJ, a considerable fraction of the alpha component of the fusion yield $Y/5 = 630$ kJ. Alpha particle energy is expected to be trapped near the capsule close to bang time due to their short range in the compressed fuel and remnant carbon ablator; the neutron component, however, escapes the hohlraum region almost unperturbed [42–44], taking 80% of the total fusion energy with it. Our observations show a large and predictable fraction of the alpha energy couples to the hohlraum a short period after peak fusion reactivity, and in the next section we will quantify the magnitude of the observed delay.

Nuclear "bang time" at NIF, is defined as the time between the initial rise of the laser drive and peak fusion reactivity, and is generally measured using the gamma reaction history diagnostic [45–48]. Across the shot series, bang times were observed between 9.25 and 9.6 ns, with later bang times corresponding to shots N220919 and N221204 which incorporated a 300 ps longer drive pulse, made possible through upgrades to the NIF laser system during 2022 [49]. To compare Dante against bang time, Gaussian fits were made to the residuals ± 300 ps either side of the highest point, with the reheating peak timing t_D defined as the centroid of the Gaussian. Figures 4(a) and 4(b) show peak Dante 1 and 2 reheating time compared with nuclear bang times respectively; both Dantes show close correlation with nuclear bang time with a systematic delay of ~500 ps and tight spread across all shots comparable to the 50 ps absolute timing uncertainty, illustrated in Fig. 4(c). The close agreement between gamma reaction history (GRH) and Dante confirms the nuclear origin, but the cause of the 500 ps offset is not immediately obvious.

A delay suggests the signal does not originate from the burning capsule directly, and that the fusion energy has been absorbed and thermalized by the hohlraum. Figure 5

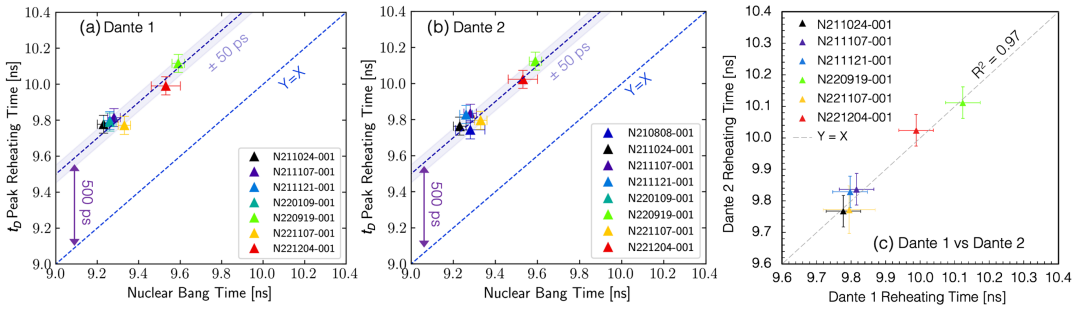

FIG. 4. (a),(b) Dante 1 and 2 reheating peaks compared with nuclear bang times from the GRH and QCD diagnostics respectively. (c) Cross plot showing the observed reheating peaks for Dante 1 and 2 with a correlation of $R^2 = 0.97$ and scatter < 50 ps, well within the absolute uncertainty of the gold ball timing measurement.

shows Dante 1 spectra generated at peak laser drive across the shot series, exhibiting the characteristic Planckian and gold *m*-band shape presented in Fig. 1(b). Also shown is the spectra at 10 ns for shot N221204, corresponding to the peak in the fusion-induced hohlraum reheating. The profile is clearly thermal, similar in shape to the spectra during the laser drive, albeit with higher total integrated power. If the reheating signal were emitted directly from the compressed core at bang time, we should expect a bremsstrahlung-like shape [4] with a sharp drop below 2 keV due to the presence of tungsten dopant in the ablator shell [50]. By combining the thermal shape and 500 ps delay, we surmise the capsule energy has undergone a series of conversion and absorption steps, ultimately leading to a quasiconventional heating of the hohlraum walls. In the following section we examine the specific processes which transfer energy from the burning capsule to the gold hohlraum walls, eventually to be measured by Dante.

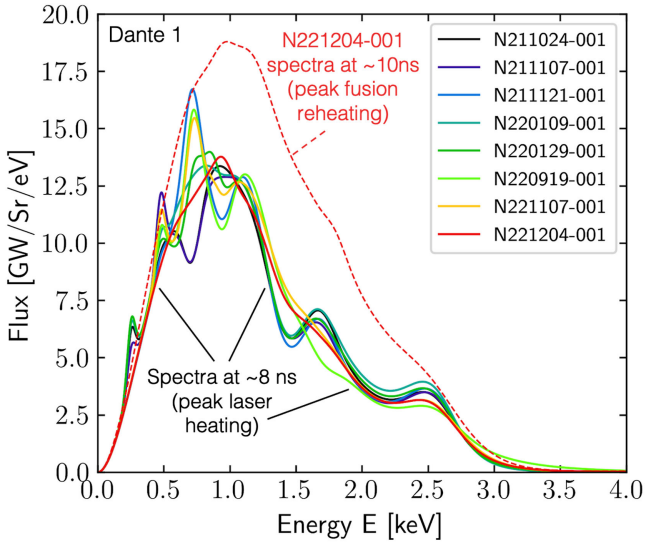

FIG. 5. Spectra from Dante 1 calculated using *UNSPEC* at peak laser drive for all shots; for comparison, the spectra from N221204 as the hohlraum is redriven by fusion energy is shown in dashed red.

The principal tool for investigating the heating process has been the ICF 2D radiation-hydrodynamics simulation code, LASNEX [51], with updated physics models that have been described in the literature [52,53]. Shot N210808 was used as a test case, with a fuel-ablator mix model adjusted to produce a capsule yield of 1.4 MJ, consistent with the observed fusion yield of 1.36 MJ. We then increase the yield in a follow-on simulation to 4.2 MJ. This is achieved by introducing an magnetohydrodynamic model [54] which includes self-generated magnetic fields in simulating the plasma and radiation environment in the hohlraum. This model produces a more spherically symmetric implosion, resulting in higher yield and allowing us to investigate how predictions evolve with increasing yield.

Simulations are postprocessed using x-ray flux tally surfaces to generate synthetic Dante flux histories, allowing direct comparison with observations. Figure 6(a) shows the resulting synthetic profiles for the 1.4 MJ and 4.2 MJ cases; the simulations clearly feature a sharp rise shortly after capsule bang time, and the magnitude of that rise increases with fusion yield. Also shown are the residual heating signatures from the simulations extracted using the methodology outlined previously; the shape, timing, and magnitude of these features in the LASNEX simulations compare well with the shot data in Fig. 3(a), with the simulation predicting 42 kJ of reheating for N210808 (vs 52 ± 12 kJ observed) at a t_D of 490 ps (vs 470 ± 90 ps observed). We can therefore, with confidence, interrogate the details of the simulations to identify the precise cause of this reheating.

The 1.4 MJ DT yield consists of 1.1 MJ of 14 MeV neutrons and 0.3 MJ of alpha particles. It is unlikely that either component can heat the walls directly. As discussed earlier, neutrons deposit only a small fraction of their energy in the imploded capsule core and mostly escape the hohlraum walls unperturbed. The alphas conversely, deposit almost all their energy in the imploded capsule core, leaving nothing left to directly interact with the gold wall. Thus, the hohlraum walls must be reheated indirectly.

We are left to consider what happens to the alpha-heated compressed core. Post bang time, electron temperatures T_e

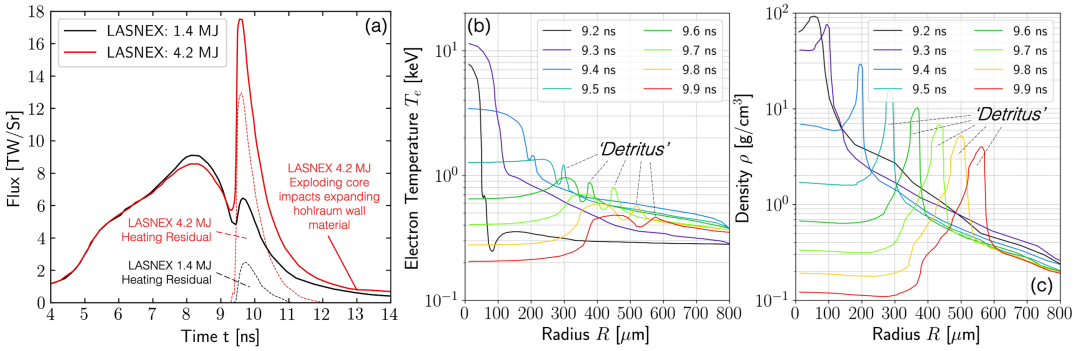

FIG. 6. (a) LASNEX calculations based on experiment N210808-001, alongside residual reheating signatures. (b) Radial electron temperature T_e snapshots between 9.2 and 9.9 ns from the LASNEX simulations showing the blast-wave heated *detritus* remains hot several 100 ps after nuclear bang time (9.25 ns), as observed by Dante. (c) Radial density ρ snapshots of the capsule between 9.2 and 9.9 ns, showing expansion after heating from the alpha heated core's expanding blast wave.

and densities in the exploding core can reach 10 keV and 100 g/cm^2 as highlighted in Figs. 6(b) and 6(c); consequently, the exploding core emits prompt x-ray radiation. Careful analysis of the simulations shows that the photons emitted during this process which can reach the hohlraum wall are high energy (> 5 keV), and these deposit deep in the gold walls, so deep, that the heating would not be observable from the Dante diagnostics, which collects photons emitted from the first optical depth of the wall surface. Lower-energy prompt x-rays < 5 keV are absorbed by the remaining tungsten-doped ablator.

Following peak compression, the imploded core relieves the ~400 Gbar of pressure by expanding into the hohlraum. Internal thermal energy is thus converted into hydrodynamic kinetic PdV energy. The hohlraum, however, is not a vacuum. In the immediate vicinity of the imploded core is the previously blown-off ablator material which drove the original compression via the rocket effect [55]. The expanding core plows into this material and partially stagnates against it, heating the blow-off material. A portion of the ablated matter impacted by the core is the original tungsten-doped ablator. The reheated tungsten-doped material impacted by the expanding core now radiates, forming the principal source of radiation that heats the inner surface of the gold hohlraum walls. It is this reheating that we observe on Dante. We choose to call this blast-wave-driven heating of the previously ablated tungsten-doped shell, and subsequent reheating of the gold hohlraum walls: *detritus drive*. Figures 6(b) and 6(c) show sequential radial lineouts of electron temperature T_e and density ρ and illustrate the time history of the blast wave stagnating on, and heating, the ablated *detritus*.

Significantly later in time, the exploding core will impact the expanding gold wall material. One could imagine this stagnation would be an effective way to generate radiation that reheats the wall. The simulation, as well as a simple analytic estimate using the sound speed of the expanding core, reveals this collision occurs several nanoseconds after bang time, and is thus not the origin of the observed reheating. It is, in fact, much weaker, and a late contributor to the Dante signal. It is barely visible in the 1.4 MJ simulation; however, the effect presents as a slight inflection at 13 ns for the 4.2 MJ simulation in Fig. 6(a). The effect can also be clearly seen in the observed Dante data from N221204 in Figs. 2(a) and 3(a), and at 13 ns, providing confidence that our simulation methodology accurately captures the physics at play. As fusion gains at NIF continue to increase in future shots, we expect this late-time wall-collision phenomenon to become increasingly prominent.

From our physics understanding described above, in the current yield regime at NIF we can derive a scaling relation for the hohlraum reheating flux observed by Dante as a function of fusion yield. As described earlier, the alpha component of the yield Y is the basic drive source for the hohlraum reheating. The energy undergoes many conversions (from thermal to PdV, back to thermal after stagnation with the *detritus*, to radiative emission), but fundamentally the radiant source of reheating is proportional to Y. This "source" is balanced by an energy sink, namely absorption into the walls. The loss can be described in terms of the wall temperature T_W achieved due to reheating; the characteristics of such losses in gold have been discussed in detail previously [56] and scale as $T_W^{3.3}$, and thus yield $Y \sim T_W^{3.3}$. The walls themselves however, will radiate conventionally at T_W^4, and it is this flux we observe from Dante. Thus, we would expect the Dante Flux signal, which scales as T_W^4 (which is identical to $T_W^{3.3\times1.21}$) to scale as $Y^{1.21}$. This is precisely the scaling of the Dante flux data with Yield that is presented in both Figs. 2(c) and 3(c), and is also the scaling predicted by the full simulations. This scaling now allows us to utilize the Dante reheating signal from future experiments as an independent indicator of fusion yield, and as a complement to existing neutron diagnostics.

In summary, we have observed for the first time substantial reheating of indirect-drive hohlraums from burning fusion capsules, at levels comparable, and exceeding, the

original NIF laser drive. As yields at NIF continue past breakeven and the hohlraum is reheated beyond the temperatures achievable by the NIF laser system alone, we can explore these unique hohlraum conditions as a driver for derivative experiments, where a rapidly driven (< 500 ps) thermal source ($T_R > 300$ eV) is useful, specifically material properties in the HED regime, such as opacity, strength, and equation of state. Comparisons of the observed Dante signals against conventional measurements of fusion yield and nuclear bang time, as well as investigations of the phenomena using LASNEX, allow us to correlate the redriven hohlraum with x-ray emissions from the remnant tungsten-doped ablator after being reheated by the exploding alpha-heated core. Hohlraum reheating was long predicted by theory and simulation, but it is only now with NIF achieving megajoule-scale yields that we have finally observed the effect in the laboratory. At this time, the Dante calorimeters are the only detectors capable of detecting the alpha component of the fusion yield, without reliance on neutron detection, thereby adding a new capability to the suite of nuclear diagnostics and lending additional credibility to future yield measurements at NIF.

This work was performed under the auspices of the U.S. Department of Energy by the Lawrence Livermore National Laboratory under Contract No. DE-AC52-07NA27344 (LLNL-JRNL-845705).

*rubery1@llnl.gov

[1] E. I. Moses and C. R. Wuest, Fusion Sci. Technol. **47**, 314 (2005).

[2] E. Moses, R. Bonanno, C. Haynam, R. Kauffman, B. MacGowan, R. Patterson, R. Sawicki, and B. Van Wonterghem, Eur. Phys. J. D **44**, 215 (2007).

[3] E. I. Moses, Fusion Eng. Des. **85**, 983 (2010).

[4] J. Lindl, Phys. Plasmas **2**, 3933 (1995).

[5] M. D. Rosen, in *Lectures in the Scottish Universities Summer School in Physics on High Energy Laser Matter Interactions, 2005* (2009), pp. 325–353, https://www.osti.gov/servlets/purl/885380.

[6] M. D. Rosen, Phys. Plasmas **6**, 1690 (1999).

[7] A. Kritcher, A. Zylstra, D. Callahan, O. Hurricane, C. Weber, J. Ralph, D. Casey, A. Pak, K. Baker, B. Bachmann *et al.*, Phys. Plasmas **28**, 072706 (2021).

[8] N. Meezan, L. Atherton, D. Callahan, E. Dewald, S. Dixit, E. Dzenitis, M. Edwards, C. Haynam, D. Hinkel, O. Jones *et al.*, Phys. Plasmas **17**, 056304 (2010).

[9] J. Lindl, O. Landen, J. Edwards, E. Moses, and N. team, Phys. Plasmas **21**, 020501 (2014).

[10] A. Kritcher, D. Clark, S. Haan, S. Yi, A. Zylstra, D. Callahan, D. Hinkel, L. Berzak Hopkins, O. Hurricane, O. Landen *et al.*, Phys. Plasmas **25**, 056309 (2018).

[11] D. Callahan, O. Hurricane, J. Ralph, C. Thomas, K. Baker, L. Benedetti, L. Berzak Hopkins, D. Casey, T. Chapman, C. Czajka *et al.*, Phys. Plasmas **25**, 056305 (2018).

[12] A. Kritcher, A. Zylstra, D. Callahan, O. Hurricane, C. Weber, D. Clark, C. Young, J. Ralph, D. Casey, A. Pak *et al.*, Phys. Rev. E **106**, 025201 (2022).

[13] A. Zylstra, O. Hurricane, D. Callahan, A. Kritcher, J. Ralph, H. Robey, J. Ross, C. Young, K. Baker, D. Casey *et al.*, Nature (London) **601**, 542 (2022).

[14] A. Zylstra, D. Casey, A. Kritcher, L. Pickworth, B. Bachmann, K. Baker, J. Biener, T. Braun, D. Clark, V. Geppert-Kleinrath *et al.*, Phys. Plasmas **27**, 092709 (2020).

[15] A. Zylstra, A. Kritcher, O. Hurricane, D. Callahan, J. Ralph, D. Casey, A. Pak, O. Landen, B. Bachmann, K. Baker *et al.*, Phys. Rev. E **106**, 025202 (2022).

[16] E. Dewald, K. Campbell, R. Turner, J. Holder, O. Landen, S. Glenzer, R. Kauffman, L. Suter, M. Landon, M. Rhodes *et al.*, Rev. Sci. Instrum. **75**, 3759 (2004).

[17] C. Sorce, J. Schein, F. Weber, K. Widmann, K. Campbell, E. Dewald, R. Turner, O. Landen, K. Jacoby, P. Torres *et al.*, Rev. Sci. Instrum. **77**, 10E518 (2006).

[18] J. L. Kline, K. Widmann, A. Warrick, R. Olson, C. Thomas, A. Moore, L. Suter, O. Landen, D. Callahan, S. Azevedo *et al.*, Rev. Sci. Instrum. **81**, 10E321 (2010).

[19] A. Moore, A. Cooper, M. Schneider, S. MacLaren, P. Graham, K. Lu, R. Seugling, J. Satcher, J. Klingmann, A. Comley *et al.*, Phys. Plasmas **21**, 063303 (2014).

[20] M. S. Rubery, G. E. Kemp, M. C. Jones, N. Pelepchan, W. C. Stolte, and J. Heinmiller, Rev. Sci. Instrum. **94**, 031101 (2023).

[21] M. Rubery, N. Ose, M. Schneider, A. Moore, J. Carrera, E. Mariscal, J. Ayers, P. Bell, A. Mackinnon, D. Bradley *et al.*, Rev. Sci. Instrum. **93**, 113502 (2022).

[22] H. Abu-Shawareb, R. Acree, P. Adams, J. Adams, B. Addis, R. Aden, P. Adrian, B. Afeyan, M. Aggleton, L. Aghaian *et al.*, Phys. Rev. Lett. **129**, 075001 (2022).

[23] O. Hurricane, in *Proceedings of the 2022 IEEE International Conference on Plasma Science (ICOPS)* (IEEE, New York, 2022), pp. 1–1, 10.1109/ICOPS45751.2022.9813006.

[24] H. Abu-Shawareb *et al.*, this issue, Phys. Rev. Lett. **132**, 065102 (2024).

[25] A. Pak *et al.*, companion paper, Phys. Rev. E **109**, 025203 (2024).

[26] A. L. Kritcher *et al.*, companion paper, Phys. Rev. E **109**, 025204 (2024).

[27] D. Pellinen and M. Griffin, Response time measurements of the NIF DANTE XRD-31 x-ray diodes (preprint), Technical Report, National Security Technologies, 2009, https://inis.iaea.org/search/search.aspx?orig_q=RN:40028874.

[28] B. Beeman, A. Moore, A. Wargo, P. Bell, W. Widmann, T. Clancy, F. Barbosa, B. Prat, and V. Allouche, in *Target Diagnostics Physics and Engineering for Inertial Confinement Fusion VI* (SPIE, 2017), Vol. 10390, pp. 14–32.

[29] K. Campbell, F. Weber, E. Dewald, S. Glenzer, O. Landen, R. Turner, and P. Waide, Rev. Sci. Instrum. **75**, 3768 (2004).

[30] M. May, K. Widmann, C. Sorce, H. Park, and M. Schneider, Rev. Sci. Instrum. **81** (2010).

[31] C. Harris, G. Kemp, M. Schneider, K. Widmann, M. Rubery, and M. May, Rev. Sci. Instrum. **92**, 033505 (2021).

[32] M. May, J. Weaver, K. Widmann, G. Kemp, D. Thorn, J. Colvin, M. Schneider, A. Moore, and B. Blue, Rev. Sci. Instrum. **87**, 11E330 (2016).
[33] N. E. Palmer, H. Chen, J. Nelson, S. Heerey, K. Piston, M. Thao, M. Schneider, P. Bell, D. Bradley, J. Porter *et al.*, in *Target Diagnostics Physics and Engineering for Inertial Confinement Fusion IV* (SPIE, 2015), Vol. 9591, pp. 33–45.
[34] J. Larsen, ICF Quarterly Report, 33'e Volume **4**, Number 4, 125 (1994), https://www.osti.gov/servlets/purl/71393#page=7.
[35] G. W. Cooper and C. L. Ruiz, Rev. Sci. Instrum. **72**, 814 (2001).
[36] G. Cooper, C. Ruiz, R. Leeper, G. Chandler, K. Hahn, A. Nelson, J. Torres, R. Smelser, B. McWatters, D. Bleuel *et al.*, Rev. Sci. Instrum. **83**, 10D918 (2012).
[37] D. L. Bleuel, C. Yeamans, L. Bernstein, R. Bionta, J. Caggiano, D. Casey, G. Cooper, O. Drury, J. Frenje, C. Hagmann *et al.*, Rev. Sci. Instrum. **83**, 10D313 (2012).
[38] R. Bionta, D. Barker, E. Casco, R. Ehrlich, J. Giemso, A. Golod, G. Grim, K. Hahn, E. Hartoni, E. Henry *et al.*, in *APS Division of Plasma Physics Meeting Abstracts* (2019), Vol. 2019 pp. TO5–004, https://meetings.aps.org/Meeting/DPP19/Session/TO5.4.
[39] K. Hahn, R. Bionta, E. Henry, D. Rusby, A. Moore, D. Barker, E. Casco, T. Golod, G. Grim, E. Hartouni *et al.*, in *APS Division of Plasma Physics Meeting Abstracts* (2021), Vol. 2021, pp. NP11–039, https://meetings.aps.org/Meeting/DPP21/Session/NP11.39.
[40] R. Bionta, G. Grim, K. Hahn, E. Hartouni, E. Henry, H. Khater, A. Moore, and D. Schlossberg, Rev. Sci. Instrum. **92**, 043527 (2021).
[41] D. Bleuel, L. Bernstein, R. Bionta, G. Cooper, O. Drury, C. Hagmann, K. Knittel, R. Leeper, C. Ruiz, D. Schneider *et al.*, in *EPJ Web of Conferences* (EDP Sciences 2013), Vol. 59, p. 13015.
[42] J. Frenje, R. Bionta, E. Bond, J. Caggiano, D. Casey, C. Cerjan, J. Edwards, M. Eckart, D. Fittinghoff, S. Friedrich *et al.*, Nucl. Fusion **53**, 043014 (2013).
[43] A. Moore, E. Hartouni, D. Schlossberg, S. Kerr, M. Eckart, J. Carrera, L. Ma, C. Waltz, D. Barker, J. Gjemso *et al.*, Rev. Sci. Instrum. **92**, 023516 (2021).
[44] E. Hartouni, M. Eckart, G. Grim, R. Hatarik, S. Kerr, A. Moore, and D. Schlossberg, in *APS Division of Plasma Physics Meeting Abstracts* (2019), Vol. 2019, pp. TO5–003, https://meetings.aps.org/Meeting/DPP19/Session/TO5.3.
[45] H. W. Herrmann, N. Hoffman, D. Wilson, W. Stoeffl, L. Dauffy, Y. Kim, A. McEvoy, C. Young, J. Mack, C. Horsfield *et al.*, Rev. Sci. Instrum. **81**, 10D333 (2010).
[46] H. Herrmann, Y. Kim, C. Young, V. Fatherley, F. Lopez, J. Oertel, R. Malone, M. Rubery, C. Horsfield, W. Stoeffl *et al.*, Rev. Sci. Instrum. **85**, 11E124 (2014).
[47] H. Herrmann, C. Young, J. Mack, Y. Kim, A. McEvoy, S. Evans, T. Sedillo, S. Batha, M. Schmitt, D. Wilson *et al.*, in *Journal of Physics: Conference Series* (IOP Publishing, 2010), Vol. 244, p. 032047.
[48] M. Rubery, C. Horsfield, H. Herrmann, Y. Kim, J. Mack, C. Young, S. Evans, T. Sedillo, A. McEvoy, S. Caldwell *et al.*, Rev. Sci. Instrum. **84**, 073504 (2013).
[49] J.-M. G. Di Nicola, T. Suratwala, L. Pelz, J. Heebner, D. Alessi, A. Bhasker, T. Bond, M. Bowers, G. Brunton, B. Buckley *et al.*, in *High Power Lasers for Fusion Research VII* (SPIE, 2023), p. PC1240103.
[50] D. S. Clark, S. W. Haan, B. A. Hammel, J. D. Salmonson, D. A. Callahan, and R. P. J. Town, Phys. Plasmas **17**, 052703 (2010).
[51] G. Zimmerman and W. Kruer, Comments Plasma Phys. Controlled Fusion **2**, 51 (1975), https://www.osti.gov/etdeweb/biblio/7214660.
[52] M. Rosen, H. Scott, D. Hinkel, E. Williams, D. Callahan, R. Town, L. Divol, P. Michel, W. Kruer, L. Suter *et al.*, High Energy Density Phys. **7**, 180 (2011).
[53] O. Jones, L. Suter, H. Scott, M. Barrios, W. Farmer, S. Hansen, D. Liedahl, C. Mauche, A. Moore, M. Rosen *et al.*, Phys. Plasmas **24**, 056312 (2017).
[54] W. Farmer, J. Koning, D. Strozzi, D. Hinkel, L. Berzak Hopkins, O. Jones, and M. Rosen, Phys. Plasmas **24**, 052703 (2017).
[55] Y. Saillard, Nucl. Fusion **46**, 1017 (2006).
[56] J. H. Hammer and M. D. Rosen, Phys. Plasmas **10**, 1829 (2003).